

Design and development of an in-line sputtering system and process development of thin film multilayer neutron supermirrors

A. Biswas, R. Sampathkumar, Ajaya Kumar, D. Bhattacharyya, N. K. Sahoo, K. D. Lagoo, R. D. Veerapur, M. Padmanabhan, R. K. Puri, Debarati Bhattacharya, Surendra Singh, and S. Basu

Citation: *Review of Scientific Instruments* **85**, 123103 (2014); doi: 10.1063/1.4902184

View online: <http://dx.doi.org/10.1063/1.4902184>

View Table of Contents: <http://scitation.aip.org/content/aip/journal/rsi/85/12?ver=pdfcov>

Published by the [AIP Publishing](#)

Articles you may be interested in

[Conformal growth of Mo/Si multilayers on grating substrates using collimated ion beam sputtering](#)

J. Appl. Phys. **111**, 093521 (2012); 10.1063/1.4710985

[Low emissivity Ag/Ta/glass multilayer thin films deposited by sputtering](#)

J. Appl. Phys. **110**, 063508 (2011); 10.1063/1.3636107

[Atomic diffusion bonding of wafers with thin nanocrystalline metal films](#)

J. Vac. Sci. Technol. B **28**, 706 (2010); 10.1116/1.3437515

[Magneto-optic properties of electron cyclotron resonance ion beam sputtered and magnetron sputtered Co/Pt multilayers](#)

J. Appl. Phys. **102**, 083906 (2007); 10.1063/1.2794713

[Mechanical and structural properties of Ni/Ti multilayers and films: An application to neutron supermirrors](#)

J. Appl. Phys. **84**, 6940 (1998); 10.1063/1.368996

JANIS

Does your research require low temperatures? Contact Janis today.
Our engineers will assist you in choosing the best system for your application.



10 mK to 800 K
Cryocoolers
Dilution Refrigerator Systems
Micro-manipulated Probe Stations
LHe/LN₂ Cryostats
Magnet Systems

sales@janis.com www.janis.com
Click to view our product web page.

Design and development of an in-line sputtering system and process development of thin film multilayer neutron supermirrors

A. Biswas,¹ R. Sampathkumar,¹ Ajaya Kumar,¹ D. Bhattacharyya,¹ N. K. Sahoo,¹ K. D. Lagoo,² R. D. Veerapur,² M. Padmanabhan,² R. K. Puri,² Debarati Bhattacharya,³ Surendra Singh,³ and S. Basu³

¹Atomic & Molecular Physics Division, Bhabha Atomic Research Centre, Mumbai 400 085, India

²Division of Remote Handling & Robotics, Bhabha Atomic Research Centre, Mumbai 400 085, India

³Solid State Physics Division, Bhabha Atomic Research Centre, Mumbai 400 085, India

(Received 29 August 2014; accepted 8 November 2014; published online 4 December 2014)

Neutron supermirrors and supermirror polarizers are thin film multilayer based devices which are used for reflecting and polarizing neutrons in various neutron based experiments. In the present communication, the in-house development of a 9 m long in-line dc sputtering system has been described which is suitable for deposition of neutron supermirrors on large size (1500 mm × 150 mm) substrates and in large numbers. The optimisation process of deposition of Co and Ti thin film, Co/Ti periodic multilayers, and a-periodic supermirrors have also been described. The system has been used to deposit thin film multilayer supermirror polarizers which show high reflectivity up to a reasonably large critical wavevector transfer of $\sim 0.06 \text{ \AA}^{-1}$ (corresponding to $m = 2.5$, i.e., 2.5 times critical wavevector transfer of natural Ni). The computer code for designing these supermirrors has also been developed in-house. © 2014 AIP Publishing LLC. [<http://dx.doi.org/10.1063/1.4902184>]

INTRODUCTION

It is well understood that the interaction of neutrons with nucleus of an atom and the similarity of wavelength and energy of thermal and cold neutrons with the length and energy scales of solid and liquids make neutron scattering an unavoidable and powerful tool in condensed matter physics experiments.^{1,2} However the main limitation in neutron scattering experiment is the low flux of the useful neutrons. The neutron flux in today's high flux research reactor and pulsed spallation neutron source are lower in several order to the corresponding photon flux from X-ray sources like synchrotron accelerators. In order to improve the flux of neutron sources enormous research is going on worldwide on reactor and spallation sources. Neutron flux at the sample position can also be increased by at least one order^{3,4} by improving the performance of different neutron optical components. One of the key neutron optical components used in the neutron scattering experiment is a neutron supermirror which transports neutrons from the source to the experimental station situated at several hundred meters away.

When thermal or cold neutrons get scattered from a medium, the medium can be approximated as an optical medium where scattering length density of neutrons defines its refractive index as follows:²

$$n = \sqrt{1 - \frac{\lambda^2}{\pi} \rho b}, \quad (1)$$

where λ is wavelength of neutron, b is scattering length of the medium, and ρ is the density.

Since refractive index of neutrons is less than 1 for most of the materials, neutrons, when they are incident at a very low grazing angle of incidence below a certain critical angle (θ_c) or critical wavevector transfer ($q_c = \frac{4\pi \sin \theta_c}{\lambda}$), on a single

layer (say) Ni film, they suffer total external reflection and the reflectivity of the layer in this region is ~ 1 , while the reflectivity falls off rapidly for $\theta > \theta_c$. A multilayer device prepared by depositing two alternate materials, having strong contrast of neutron scattering length densities, creates high reflectivity Bragg peaks even beyond the critical angle or critical q value. Due to their strong contrast in scattering length densities, Ni and Ti pairs are generally preferred in fabrication of such multilayer devices for applications in neutron delivery system. A supermirror, on the other hand, is a thin film non periodic multilayer device of hundreds of alternate layers of two materials, like Ni and Ti, having contrast in their neutron scattering length densities, where the thickness of a bilayer or the d -value of the multilayer gradually increases from the substrate to the top of the device. A supermirror can thus be conceived as a stack of several multilayers having their individual Bragg peaks whose positions vary continuously and the closely spaced superimposed Bragg peaks push the critical angle of total external reflection by a large extent compared to a single layer film.⁵ The performance of the supermirror is generally described by its ‘‘ m -value’’ which is actually the ratio of critical angle of total external reflection of the supermirror to the critical angle of natural Ni, viz., ($m = \frac{\theta_c^{SM}}{\theta_c^{Ni}}$), and the flux gain due to this supermirror in the neutron guide tube is proportional to $\sim m^2$. By increasing the m -value of the supermirror not only the fluxes of the transmitted neutrons increase but also the shorter wavelengths are transmitted which opens up the availability of thermal neutrons for experiment. Moreover, by depositing a supermirror on elliptical or parabolic surface neutrons can be focused on a small sample.⁶

Thin film multilayer supermirrors where the alternate layers are ferromagnetic and nonmagnetic can also be used to polarize neutrons and in that case it is called a supermirror polarizer. For a magnetic material the expression for

refractive index is modified as follows:

$$n = \sqrt{1 - \frac{\lambda^2}{\pi} \rho(b \pm p)}, \quad (2)$$

where p is the magnetic scattering length.

The combination of the two materials (1 and 2) will be such that in the presence of magnetic field parallel to the film surface, the neutron spin parallel to the magnetization will see very large neutron scattering length contrast (i.e., $b_1 + p \gg b_2$) between the alternate layers and reflectivity of the supermirror for these neutron will be very high. However neutrons having spin anti-parallel to the magnetization will have negligible neutron scattering length density contrast between the alternate layers (i.e., $b_1 - p \approx b_2$) and they will pass through the supermirror with very low reflection. Co/Ti, Fe/Si, Fe/Ge, FeCoV/TiN are some of the commonly used material combinations of magnetic/non-magnetic layers for realizing thin film supermirror neutron polarizer or analyzer for studying the magnetic property of materials and inelastic neutron scattering experiments.⁷⁻⁹

It should be noted that for obtaining optimum performance from these devices, multilayers with low interface roughness, low inter-diffusion, and bulk-like density of the individual layers are prerequisites. It should also be noted that since the supermirrors described above reflect neutrons at very small grazing angles of incidence, their sizes need to be large enough to cover the whole incident beam from a neutron source and for actual deployment in a real experiment these devices are required in large numbers.

Mezei^{5,10} first demonstrated the design and fabrication of Fe/Ag neutron supermirror polarizer using electron beam evaporation method. However, it is now well established that in an evaporation process, due to low adatom energy of the evaporants, adatoms do not get sufficient energy to reorient themselves on the surface of a growing film and films thus preferably grow in a columnar fashion which prevents realization of low interface roughness in these multilayers. On the contrary, in a sputtering technique, the energy of the adatoms is generally high enough (~ 10 eV) so that adatoms can reorganise themselves on the surface of the growing films leading to smoother two-dimensional growth. Hence, presently different variants of sputtering technology are generally used to realize these multilayers. Some of the researchers^{6,11,12} have reported deposition of very large m -value supermirrors by Ion Beam Sputtering (IBS) technique. In spite of several advantages of IBS technique like low air pressure plasma, higher stability of process, and noncontact of plasma with deposited film, IBS technique is not suitable for large area and high throughput deposition due to the enormous cost involved in procurement of large size ion guns and low deposition rate of the ion beam sputtering process. DC magnetron sputtering which can yield higher sputtering rate and which has easy scalability and provisions for reactive sputtering in various gaseous ambient is thus a preferred technique for depositing these multilayers neutron supermirrors for actual applications.

Several workers have reported the advantage of reactive sputtering technique in realization of good quality neutron supermirrors. Elsenhans *et al.*¹³ have demonstrated the favorable effect of using N_2 during deposition of Ni in Ni/Ti su-

permirror, Hoghoj *et al.*¹⁴ have shown the effect of N_2 during deposition of Si in Fe/Si neutron supermirror polarizer, Senthil Kumar *et al.*¹⁵ have shown the effect of dry air during the deposition of Ni in Ni/Ti supermirror. In all these cases the reactive sputtering process is found to decrease the interface roughness of the multilayers. However, Ju and Heuser¹⁶ have reactively sputtered Ti with H_2 in order to increase the contrast between Ni and Ti in Ni/Ti monochromator. All of the above reports strongly support the use of reactive magnetron sputtering technique for deposition of neutron supermirrors. Moreover, using an in-line technique, the deposition of the multilayers on large size or large number of substrates can be easily carried out using magnetron sputtering.

In the present communication, we describe an in-house developed in-line DC reactive magnetron sputtering system and optimization of process parameters to obtain high m -value Co/Ti multilayer supermirror neutron polarizers in this system. Though there are some reports on optimization of process parameters for neutron supermirror polarizers,^{14,15,17-20} reports on the details of process development and optimization of an in-line sputtering system for development of large area supermirrors are scanty. Though the initial development of the Co/Ti supermirror polarizer using electron beam evaporation method¹⁸ has been reported, deliberations on the development of Co/Ti supermirror by magnetron sputtering technique are not available in the literature. Co/Ti is a very unique material combination for fabrication of supermirror polarizer due to its polarizing capability at low angles as pointed out by Stewart *et al.*⁸ since $-ve$ scattering length densities of Ti and Co for spin down neutrons do not support the total external reflection phenomena. Though the use of this material combination is limited by the fact that Co strongly activates in intense neutron flux environment, it can be used as analyzer⁸ at neutron flux $\sim 1.5 \times 10^6$ n cm⁻² s⁻¹ in neutron experiments, where it can isolate the spin of neutrons at very small grazing angles of reflection which other material combinations like Fe/Si fail to do.

It should be noted that though in this communication, the process of development of Co/Ti supermirror using in-house developed inline sputtering system has been described, the similar system and mechanism can also be applied for development of process for deposition of neutron supermirror of other material combinations like Ni/Ti, Fe/Si, etc.

IN-LINE DC MAGNETRON SPUTTERING SYSTEM DEVELOPMENT

In Fig. 1 the schematic of the 9 m long cylindrical coating system which is designed and built indigenously is shown. In this deposition system uniform deposition can be obtained on substrates up to 1500 mm \times 150 mm size in sputter down configuration. The system is comprised of two chambers, the first is the load lock chamber of 450 mm diameter, which is used for loading/unloading and cleaning of the substrates, while the second chamber is the main deposition chamber of same diameter. The two chambers are connected to two separate turbomolecular pumping systems and isolated by a large gate valve. In the first chamber, the substrate is loaded on a substrate trolley and is cleaned by glow discharge

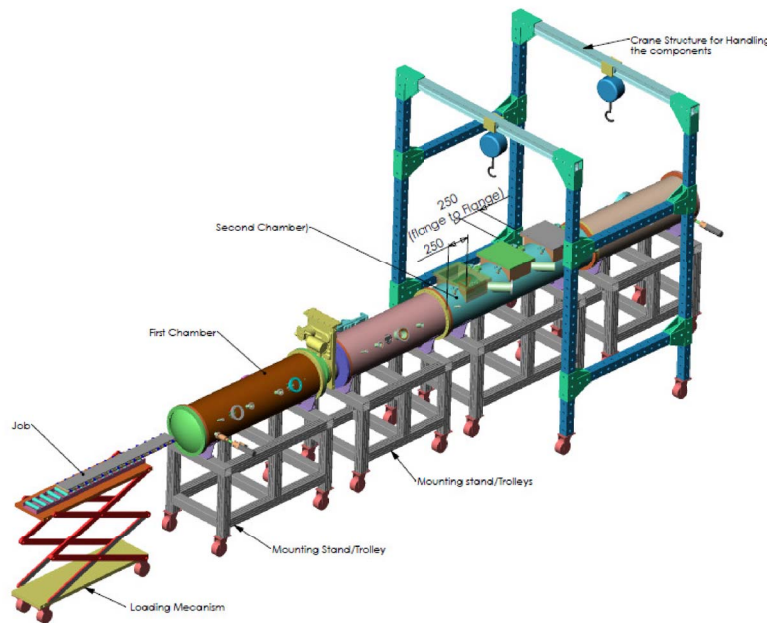
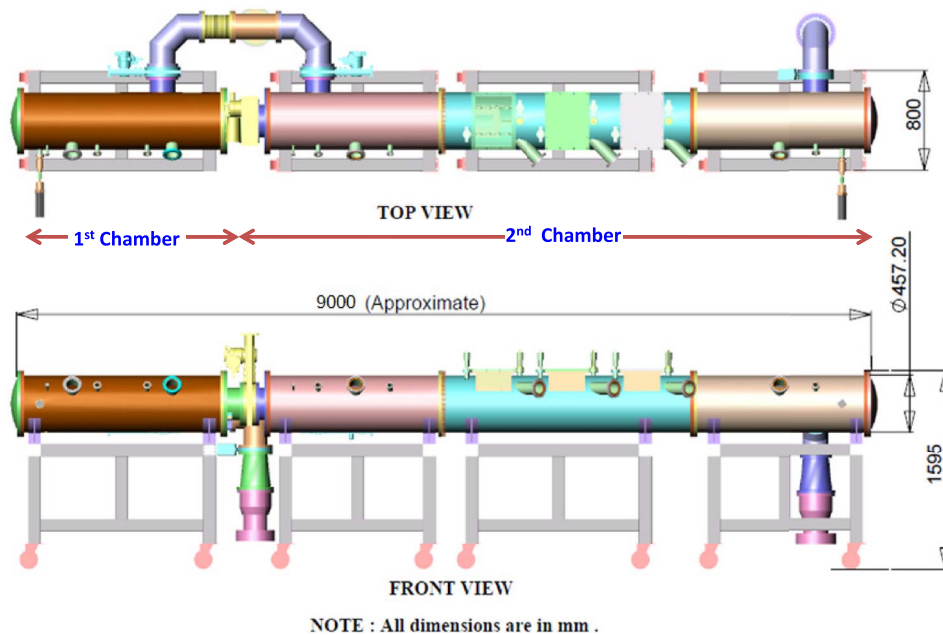


FIG. 1. Schematic diagram of the in-house developed 9 m long magnetron sputtering system.

cleaning method using a 13.56 MHz commercial RF power supply. Subsequently, the substrate is transferred to the second chamber and the gate valve between the chambers is closed.

The second chamber where the actual deposition is carried out has three compartments. As shown in the expanded view in Fig. 2, in the middle compartment three rectangular magnetron cathodes are mounted where three sputtering targets, each having dimensions of 125 mm × 200 mm, are fixed. The actual sputtering process takes place in this compartment, while the other two compartments of the second chamber act as dummy space so that the large substrate trolley can undergo a full to-and-fro motion below the target during deposition. In front of each target there is a shutter assembly, comprising of two stainless steel plates fixed in a stainless steel shaft which

move in opposite directions by two motors for opening and closing operations. Just beside each target one quartz crystal monitor with specially fabricated sputtering head sensor is fixed in the shadow region for *in situ* monitoring of the static rate of deposition. Each cathode is connected to a 2 kW dc power supply for generating plasma. In order to visualize the plasma from outside, three viewing ports are mounted on the chamber wall one near each target at an angle as shown in Fig. 2.

During any deposition, the substrate trolley is moved from one side of the second chamber to the other side with a constant predefined speed in order to deposit the whole substrate uniformly. This motion of the substrate trolley is the most critical component of this type of in-line deposition system and hence the motion assembly has been designed very

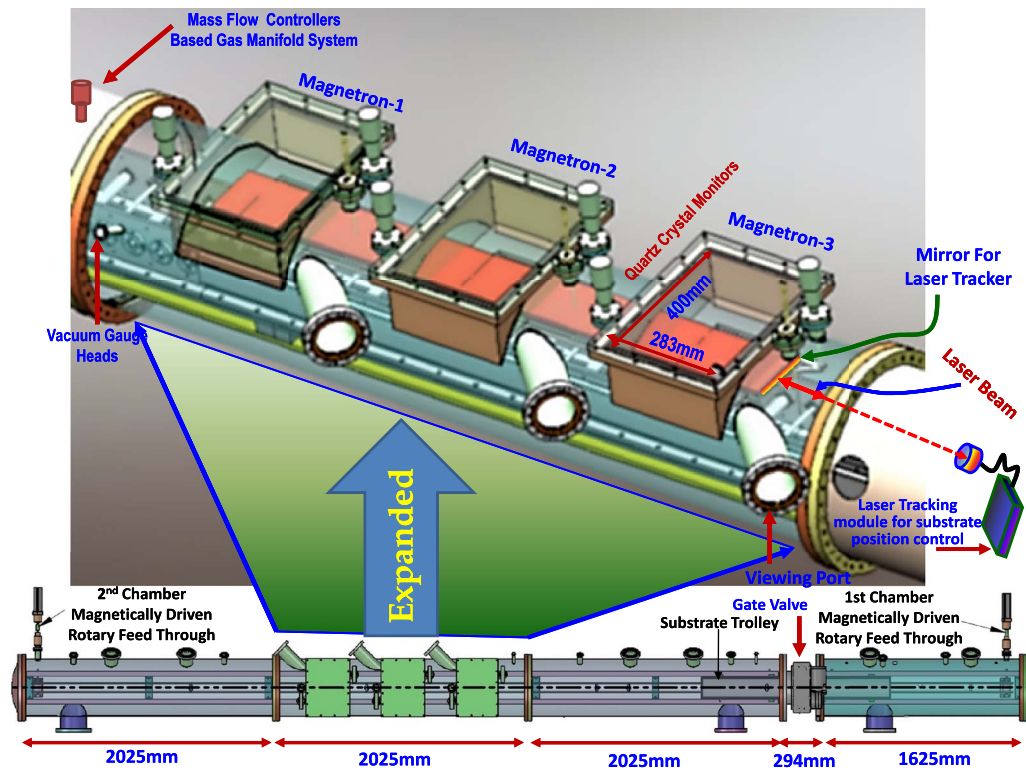


FIG. 2. Schematic diagram of the sputtering system with expanded view of the sputtering chamber along with various gadgets.

carefully to achieve jerk-free and continuous motion. After testing various options, the stainless steel rope based pulley system is chosen where two pulleys are mounted on the opposite ends of each chamber, as shown in Fig. 3. At one end, the pulley is connected with a stepper motor placed outside the vacuum chamber and interfaced to the assembly inside through a magnetically driven rotary feedthrough. Two parallel stainless steel ropes are tightly fastened over the pulleys and a small guiding trolley is fixed with the rope. Thus, being driven by the stepper motor, when the pulley rotates, the rope moves and the small guiding trolley moves over a fixed rail. The guiding trolley is clamped with the big substrate trolley and thus the substrate trolley also moves guided by bearings on side rails on both sides. The spring-loaded clamp between the guiding trolley and the substrate trolley automati-

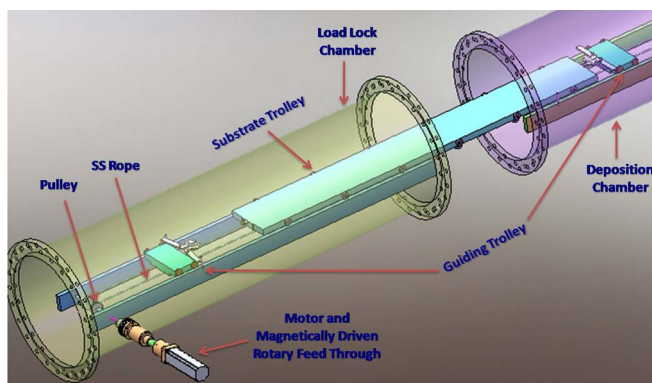


FIG. 3. Schematic diagram of the rope and pulley based substrate translation mechanism.

cally locks/unlocks at the end of both chambers when the substrate trolley is to be transferred from the first chamber to the second chamber and vice-versa. Fig. 3 shows the position of the two guiding trolleys and the large substrate trolley during automatic transfer of the substrate trolley from the deposition chamber to load-lock chamber.

During deposition, in order to track the exact position of the substrate trolley a laser based distance tracker has been fixed just outside the glass view port of one end of the deposition chamber as shown in Fig. 2. The laser beam of the distance tracker passes through the view port and gets reflected back from the substrate tray and thus the exact position of the tray inside the chamber at any point of time during deposition can be measured within an accuracy of 1 mm. The read out of the laser tracker is fed-back to the motion mechanism in a closed loop control. It should be noted here that in the above system, the design of the pulley based substrate trolley movement mechanism has been done in such a way so that an accuracy of substrate positioning within ± 0.1 mm can be achieved. However, to check the repeatability of the substrate trolley movement, several single layer films have been deposited under similar deposition conditions and it has been found that it is possible to deposit films in this system with less than 0.5% thickness error. This confirms the high mechanical repeatability of the substrate trolley movement mechanism of the coating system.

As discussed earlier, for development of neutron monochromator and supermirror, reactive sputtering sometimes becomes essential where depositions are carried out under a mixed ambient of various gases. In order to meet this requirement, a gas manifold system has been designed so that

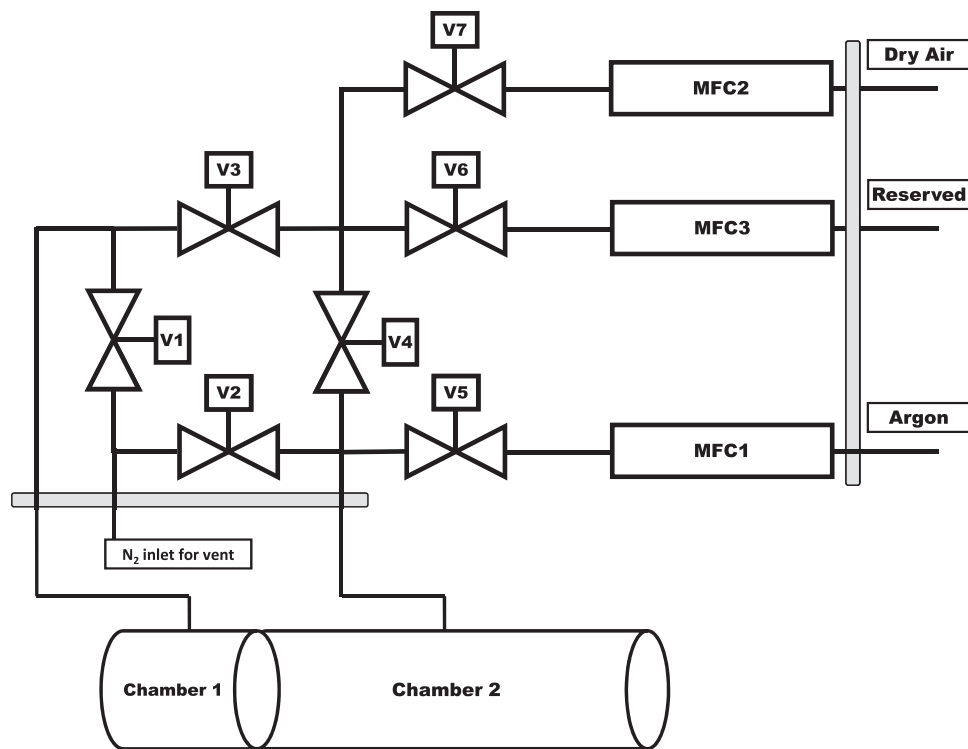


FIG. 4. Schematic lay-out of the automatic gas manifold system for reactive sputtering.

up to three gases can be mixed at a predefined ratio and can be used as ambient during the deposition. As shown in Fig. 4, three Mass Flow Controllers (MFC) and seven pneumatically controlled normally closed valves are used in the gas manifold system. The fully computer-controlled manifold system helps in choosing a mixed ambient or pure argon ambient as per the requirement, since in neutron supermirror deposition, often one layer of the bilayer stack is deposited under pure argon ambient and the other layer is deposited under mixed ambient of argon/oxygen, argon/nitrogen, or argon/hydrogen. The gas manifold has been designed in such a way that when gas mixing is not required, one of the gas (nitrogen, air, or hydrogen) can be diverted to the load-lock chamber and the MFCs are not disturbed. This methodology saves the stabilization time

(normally 5–10 s) of the MFCs starting from the closed state which has a significant cumulative effect in time management for a neutron supermirror fabrication that generally involves deposition of more than 500 layers.

PROCESS AUTOMATION FOR MULTILAYER DEPOSITION

A LabVIEW based process automation software has been developed for the fabrication of neutron supermirrors by sequential deposition of two alternate layers up to 1000 layers or so. As shown in Fig. 5, the top level Graphical User Interface (GUI) sequences the interactions with various sub systems such as micro controller based motion controller, laser

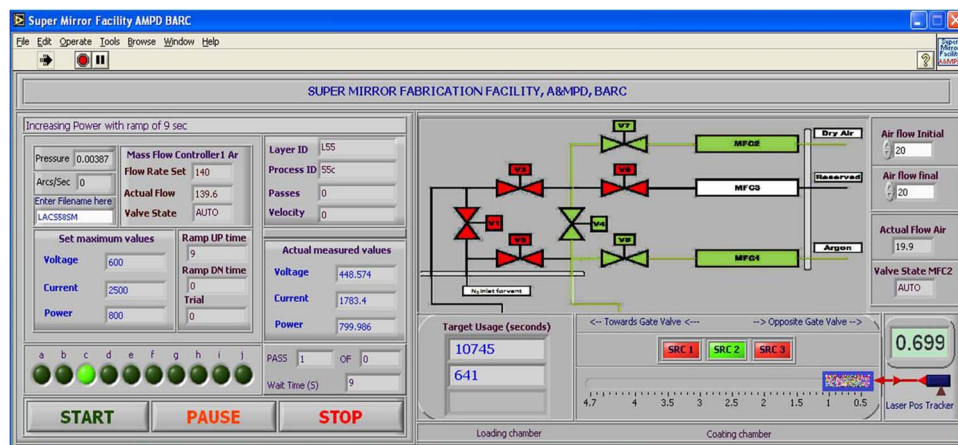


FIG. 5. Snapshot of the GUI of LabVIEW based automation program for multilayer deposition.

position tracker for substrate movement, mass flow controllers for monitoring and controlling various gas flow, DC power supplies for plasma generation, Quartz Crystal Micro balance based deposition rate, thickness and crystal life monitor, motorised shutters, microcontroller based gas manifold system, and vacuum gauges.

Each deposition process has been divided into 11 sub-processes, viz., (i) opening of the required set of electro-pneumatic valves of the gas manifolds, (ii) initialization of mass flow controllers and setting up of the required flow rate, (iii) setting up of the upper limits of voltage, current, and power, (iv) ramping up of power to the desired level at the set rate, (v) waiting for stabilization of power, (vi) setting up of final gas flow rate through MFC, (vii) logging of the process parameters prior to deposition, (viii) putting on the substrate motion at a predefined speed, (ix) opening up of the shutters and performing deposition by shuttling the substrate for a set number of passes at the set speed, (x) closing of shutters, (xi) logging of the post deposition data, (xii) decreasing magnetron power at the set ramp down rate, and (xiii) preparing for the next layer by appropriately closing the opened valves and allowing time for residual gases in the chamber to flush out. All these sub processes are depicted via a front panel mimic at every stage and deposition is carried out for the set number of layers.

The process control software runs these sub processes as set in a process table that is automatically generated from the inputs given by the user in two other tables. The material property table lists the properties specific to the material of the plasma source such as the voltage, current, and power to be applied for plasma generation and the layer information table lists the number of layers and various layer specific parameters such as layer thickness, number of passes, speed of substrate movement, flow rate of Argon and other gases, etc. Once these two tables are set, the user has to only run the process control program and click on the start process button after setting the file name for data logging. However, during the course of deposition, an option has been given to the user to modify the process parameters and restart the process at any time for offsetting cumulative process errors.

The automation is implemented by employing in-house developed interface modules for the different components, viz., (i) substrate trolley movement mechanism, (ii) laser tracker system, (iii) mass flow controllers, (iv) pneumatic valves and relays of the gas manifold system, (v) quartz crystal monitors, (vi) magnetron power supplies, and (vii) vacuum gauges that implement communication employing RS232 interface. For this purpose a 1:8 MOXA serial port extender and a 1:16 USB to serial port HUB were installed for coupling the above sub systems with the control PC. With the development of this fully automated system multilayer super mirrors having more than 500 layers with graded thickness could be fabricated in a single go at a relatively short span of time making it possible to conduct more fabrication trials under different process conditions. This ultimately helps in arriving at the best choice of process parameters for fabrication of super mirrors with the desired optical and polarization properties.

PROCESS DEVELOPMENT FOR Co/Ti SUPERMIRROR POLARIZER

Subsequent to installation of all the vacuum components and various other gadgets, leak testing of the in-line sputtering system with the helium leak detector has been carried out up to a leak rate of 10^{-10} Torr $l\ s^{-1}$, which ensures achievement of base pressure of 5×10^{-7} mbar regularly in the system. Initially, gas flow rates were optimized so as to obtain sustainable plasma with no arcing and the optimized gas flow rates of $40\ ml\ min^{-1}$ and $100\ ml\ min^{-1}$ have been obtained for Ti and Co, respectively. The flow rates are different for the two elements as ions in the plasma behave differently for the nonmagnetic and magnetic targets fixed on similar magnetron cathodes. In these flow rates, stable and uninterrupted plasma has been observed and several films have been deposited at different dc power levels at a constant substrate trolley speed of $34\ mm\ s^{-1}$. The films deposited have been characterized by measuring grazing incidence x-ray reflectivity (GIXR) spectra at $1.54\ \text{\AA}$ wavelength and the thickness, density, and top surface roughness have been estimated. In Fig. 6(a) the variation of thickness of Ti films deposited per pass of the substrate trolley with cathode power is shown. It is clear from this figure that the rate of deposition increases linearly with cathode power which confirms the linearity of this plasma system. In Fig. 6(b) the top surface roughness and the total thickness of the above films deposited at different dc power levels are shown which shows that we are able to deposit

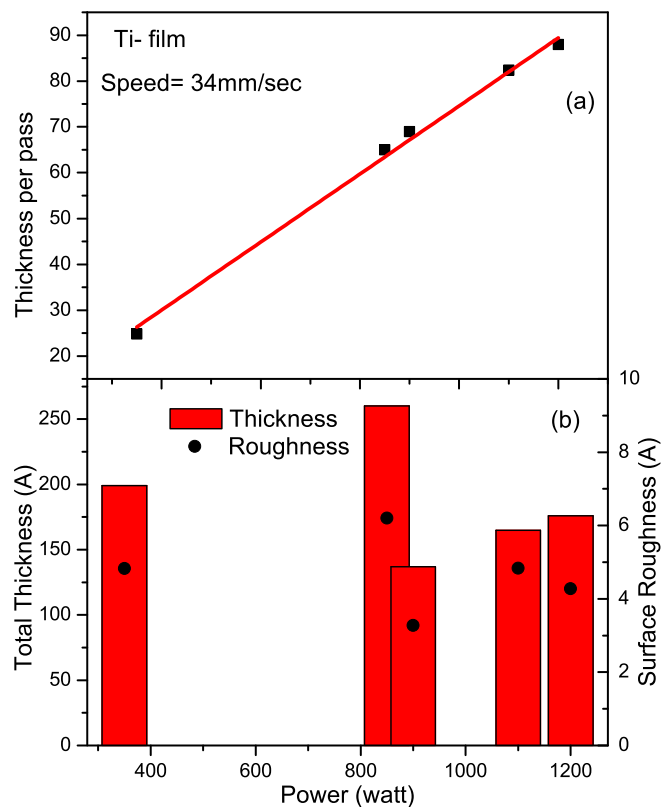


FIG. 6. (a) Variation of thickness of Ti films deposited per pass of substrate trolley as a function of magnetron power along with least square linear fit. (b) Variation of top surface roughness of Ti films as a function of magnetron power.

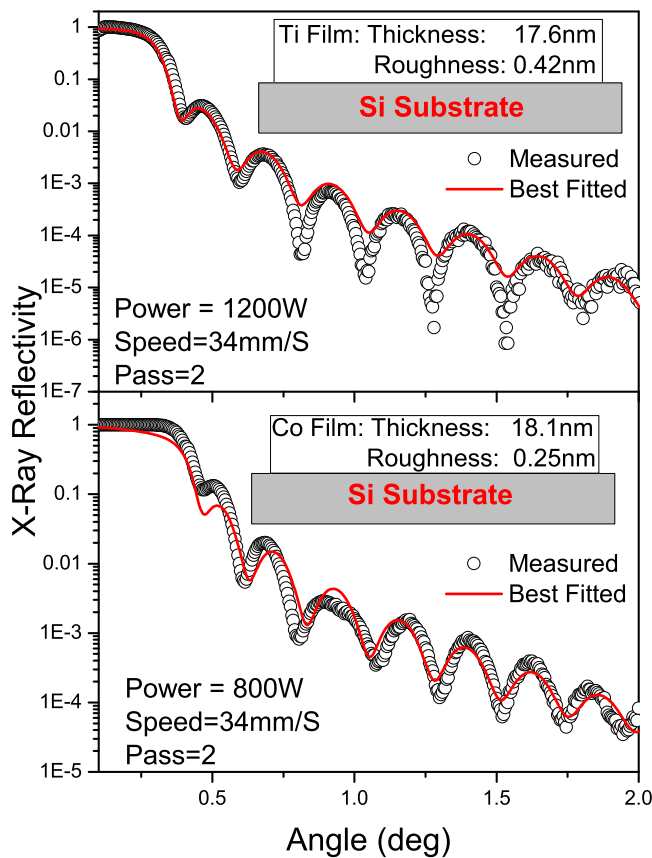


FIG. 7. GIXR spectra along with best fit theoretical spectra of Ti and Co films deposited at optimized deposition conditions.

very low roughness films using the present deposition system which is very important for the fabrication of thin film multilayer neutron optical devices. It further shows that roughness does not increase in proportionality to the thickness of the films which implies two-dimensional noncolumnar growth of the films.

Subsequently, the dc power levels of the magnetron cathodes have been optimized for both Co and Ti. The consideration of this optimisation has been the ability to deposit minimum thickness of the films per pass of the substrate trolley which is a requirement for high m -value neutron supermirror where films of very low thickness have to be deposited. The time spent in each pass of the substrate trolley is again governed by the lower and upper limits of its speed for having smooth and jerk-free motion. The optimized power of deposition for Ti films has been found to be 1200 W, while that for Co films is found to be 800 W. In Fig. 7, the GIXR spectra of the Ti and Co films deposited at these selected powers with 34 mm s⁻¹ substrate trolley speed and two passes of the substrate trolley are shown along with their best fit theoretical spectra.

The thickness uniformity achievable in this system over large area has been estimated by depositing Ti layer on several small c-Si substrates each of ~ 30 mm \times 20 mm dimensions placed on slots spreading over the length and breadth of the substrate holder covering an area of 1500 mm \times 150 mm. Single layer Ti films have been deposited on these substrates and subsequently have been characterized by GIXR technique.

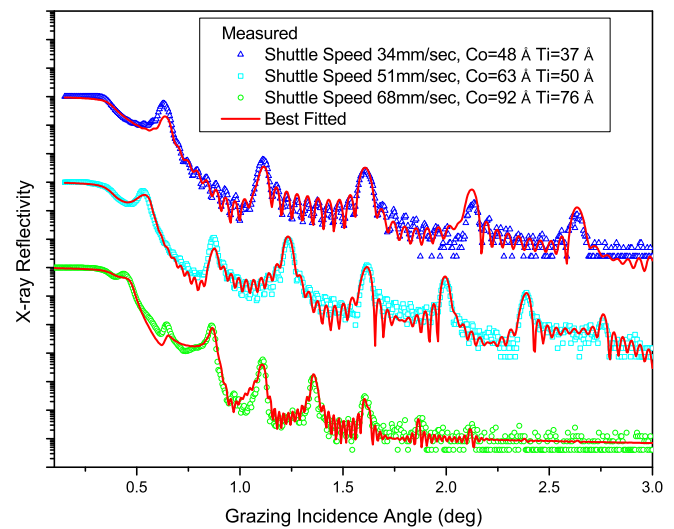


FIG. 8. GIXR spectra of 20 layer Co/Ti periodic multilayer samples deposited at three different substrate trolley speeds, viz., 34 mm s⁻¹, 51 mm s⁻¹, and 68 mm s⁻¹ along with best fit theoretical spectra.

The thickness uniformities over the 1500 mm length are found to be within $\pm 3.5\%$ and over the 150 mm width is within $\pm 4.8\%$. The detailed results have been presented in an earlier communication.²¹

Subsequently, the thickness of the films deposited has been calibrated with the speed of the substrate trolley. This is essential for the selection of speed and number of pass of the substrate trolley required for a particular layer during fabrication of a multilayer supermirror. Three 20 layers Co/Ti periodic multilayers have been deposited with three different substrate trolley speeds, i.e., 34 mm s⁻¹, 51 mm s⁻¹, and 68 mm s⁻¹, respectively in which every layer of Co and Ti is deposited by a single pass of the substrate trolley. In Fig. 8, GIXR spectra of the above three periodic multilayer samples are shown along with their best fit theoretical spectra. By fitting the experimentally measured spectra thickness of every layer, top surface roughness and interface roughness are estimated. In Fig. 9(a), the measured thicknesses of individual layers of Co and Ti are plotted with inverse of trolley speed. In both the cases it can be seen that the dependence is linear which again establishes the reproducibility of the deposition system. The slope of the linear curve gives the dynamic rate of deposition at this condition, for Co it is found to be 2987.1 Å mm s⁻¹ and for Ti it is found to be 2652 Å mm s⁻¹. As shown in Fig. 9(a), the intercept of the straight line on the zero speed⁻¹ axis is +4.21 Å for Co and -2 Å for Ti. Similar observations have also been found by Hoghoj *et al.*¹⁴ for Fe/Si periodic multilayer by GIXR technique and Houdy *et al.*²² for W/Si multilayer by ellipsometric technique. This offset, known as the “growth offset” arises due to the interdiffusion at the interface of Co and Ti and the opposite signs of growth offset for Co and Ti are due to the asymmetry of diffusion at the Co-on-Ti and Ti-on-Co interfaces. The diffusion of one material into the other is controlled by relative values of surface free energy of the materials. As Ti has lower surface free energy of 2.1 J/m² than 2.5 J/m² of Co, Co diffuses more at the Co-on-Ti interface compared to Ti at

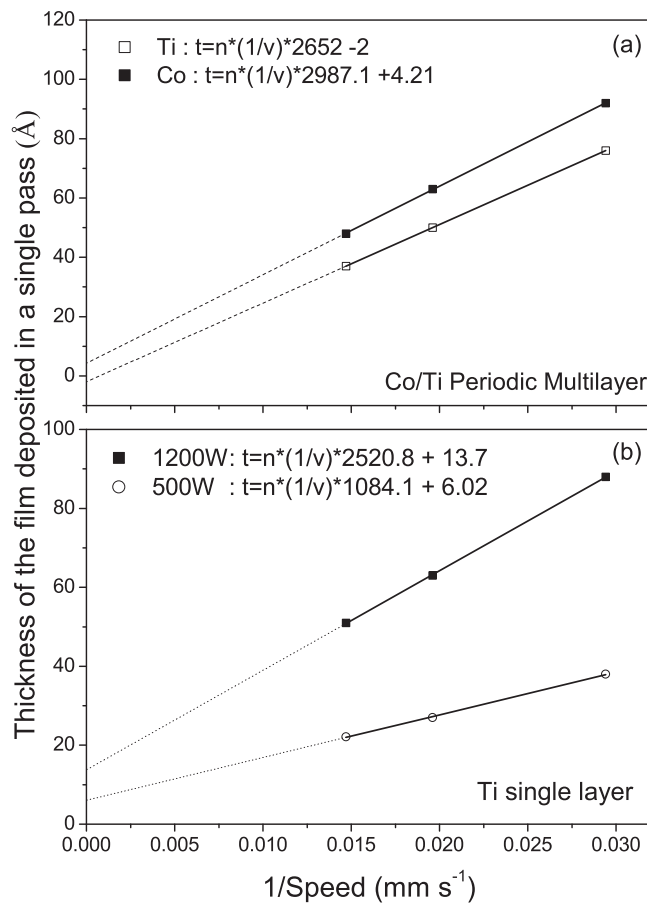


FIG. 9. Measurement of dynamic rate and growth off-set for (a) Co and Ti layers in Co/Ti multilayer and (b) Ti in single layer film deposited on Si substrate.

Ti-on-Co interface. This phenomenon decreases the effective thickness of Ti in the multilayer structure and increases the effective thickness of Co. Similar phenomena of asymmetric diffusion have also been found in our previous reports on ion beam sputtered deposited W/Si multilayer²³ and RF sputtered Ni/Ti multilayer.²⁴

In order to investigate the initial growth of Ti film, similar experiments have been carried out for single layer Ti film deposited on crystalline Si (111) substrate at two different dc power (i.e., at two different rates of deposition) levels keeping all the other parameters same. In Fig. 9(b), thickness of two set of single layer Ti films has been plotted as a function of speed⁻¹. In both the cases linear relations have been found which again confirm the repeatability of the deposition system. The dynamic deposition rates found for 1200 W and 500 W dc power levels are 2520.8 Å mm s⁻¹ and 1084.1 Å mm s⁻¹, respectively, and the growth offsets are 13.7 Å and 6.02 Å, respectively. The higher dynamic deposition rate for 1200 W is due to increase in rate of deposition which is well understood for sputtering. On the other hand, the positive values of growth off-set signifies that for both the dc power levels, the initial rate of growth of the film, i.e., just adjacent to the substrate surface is higher compared to the region away from the substrate surface. This may be due to the trapping of voids during initial growth of Ti film on the Si(111) substrate, as in this case, island-like growth is more favorable

than layer by layer growth. Similar observations have been made by Yang *et al.* in case of Ge film,²⁵ where ellipsometric measurements show different optical constant of the material at the film-air interface and at the film-substrate interface which has been attributed to trapping of voids during the initial growth of the film which creates the growth off-set as shown in Fig. 9(b). The higher value of growth off-sets for 1200 W power in this case may be due to higher rate of deposition. This higher value of growth off-set obtained at higher power suggests that for depositing very low thickness films, lower magnetron power with low speed of substrate trolley is more preferable compared to high substrate speed and higher magnetron power for this in-line sputtering system.

DEVELOPMENT OF COMPUTER CODES FOR DESIGN AND SIMULATION OF NEUTRON SUPERMIRROR AND NEUTRON SUPERMIRROR POLARIZER

After optimizing the process parameters for Co, Ti and establishing the calibration between speed of the substrate trolley and thickness deposited, the deposition of multilayer supermirrors has been initiated. To design the supermirrors, a GUI based user-friendly computer code has been developed in-house. Design of neutron supermirror had been proposed first by Mezei¹⁰ following design procedure of a broad band filter for visible optics, where thickness of the j th layer in a neutron supermirror has been proposed to be proportional to $j^{-1/4}$. However, later it was realised that this design structure is not appropriate for obtaining high reflectivity in neutron supermirrors and subsequently alternative models have been proposed by various authors.²⁶⁻³¹ Among the above models the most widely used method is by Hayter and Mook,³⁰ which is based on a discontinuous nature of variation of bilayer thickness across the supermirror structure contrary to the continuum approach of Mezei.¹⁰ The computer code discussed in the present work has been developed based on the Hayter and Mook model.³⁰

In this model, the contribution of reflectivity of each bilayer in a nonperiodic multilayer stack is calculated. Successively, the reflectivity of the k th bilayer has been matched with the $(k - 1)$ th bilayer at half intensity point. This equation has been solved by Newton iteration method and the bilayer thicknesses are calculated. Subsequently, thicknesses of the individual layers are estimated from the bilayer thickness in such a way that each layer thickness is a $\lambda/4$ plate for that particular angle of incidence. In this process, the complete supermirror structure has been designed layer by layer starting with a suitable condition and terminating at the required bilayer thickness for the desired m -value of the supermirror.

The above code has also been extended to design neutron supermirror polarizer and it has been tested by designing different supermirror and supermirror polarizers based on Ni/Ti, Co/Ti, and Fe/Si multilayers for different m values. In order to simulate the neutron reflectivity spectrum of a supermirror structure and to fit with the experimentally measured spectra, a computer code has also been developed using the Parratt's formalism.³² This code can be used to generate the polarized and nonpolarized neutron reflectivity spectrum of bulk

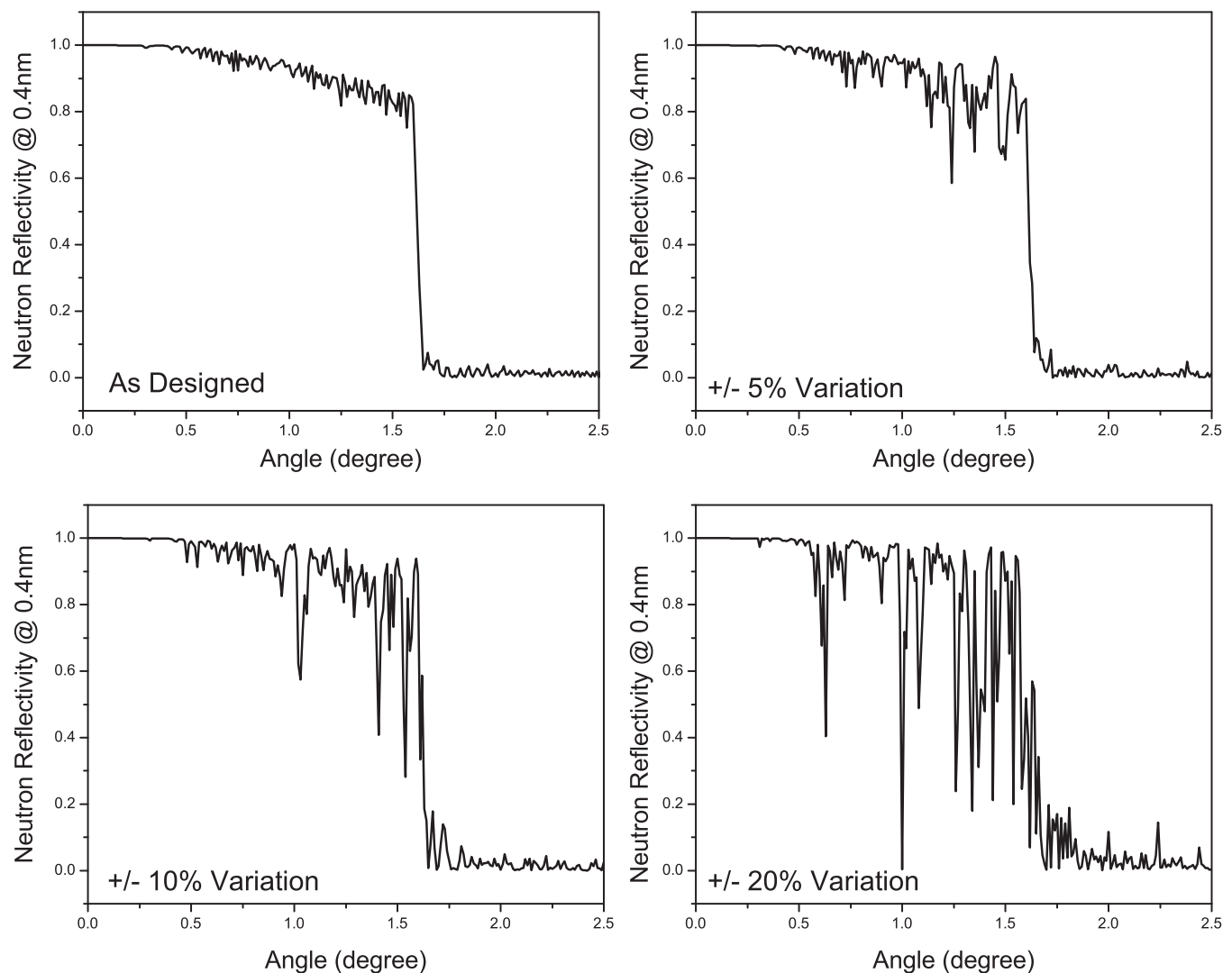


FIG. 10. Comparison of neutron reflectivity of designed Ni/Ti supermirror with $\pm 5\%$, $\pm 10\%$, and $\pm 20\%$ thickness errors.

material, single layer films, and any type of multilayer structure of periodic and nonperiodic type such as multilayer supermirror polarisers. Interface diffusion and interface roughness at the different bilayers can be included in the simulation. Neutron reflectivity patterns of supermirror structures with random and specific thickness errors can also be generated using this code. Neutron reflectivity of a Ni/Ti supermirror with $\pm 5\%$, $\pm 10\%$, and $\pm 20\%$ thickness errors have been generated and the reflectivity profiles simulated with 4 \AA neutron wavelength of these supermirrors with that of an ideal supermirror are compared in Fig. 10. It is observed that more than $\pm 5\%$ thickness error drastically deteriorates the optical performance of a neutron supermirror. In the in-line sputtering system, described in this work, this thickness uniformity is mainly controlled by the mechanical repeatability of the substrate trolley motion mechanism and hence significant effort has been given to improve this.

The effect of reflectivity of a supermirror due to some missing layers during the deposition process is also analysed and it is seen that even a single missing layer affects the performance drastically. The above in-house developed custom-made code has been very useful to estimate the process er-

rors that might have been occurred during deposition of a multilayer supermirror, from the post-deposition analysis of its neutron reflectivity pattern. It should be noted that such a computer code is not available commercially and it is very useful not only to design the structure and simulate the neutron reflectivity pattern but also in reverse engineering during the process optimization.

DEPOSITION OF HIGH m -VALUE Co/Ti MULTILAYER NEUTRON SUPERMIRRORS

Supermirror polarizers of $m = 2.0$ (100 layers), $m = 2.25$ (204 layers), and $m = 2.5$ (312 layers) have been designed using the above computer code, the material property table and the layer information table have been generated and the multilayers have been deposited using the above automatic in-line dc sputtering system. The depositions have been carried out using the in-house developed process control software described above on $240 \text{ mm} \times 140 \text{ mm}$ substrates with 6 substrates loaded at a single shot. Fig. 11 shows the nominal values of the layer structures of the above three supermirrors as obtained by our design code. Subsequent to the deposition,

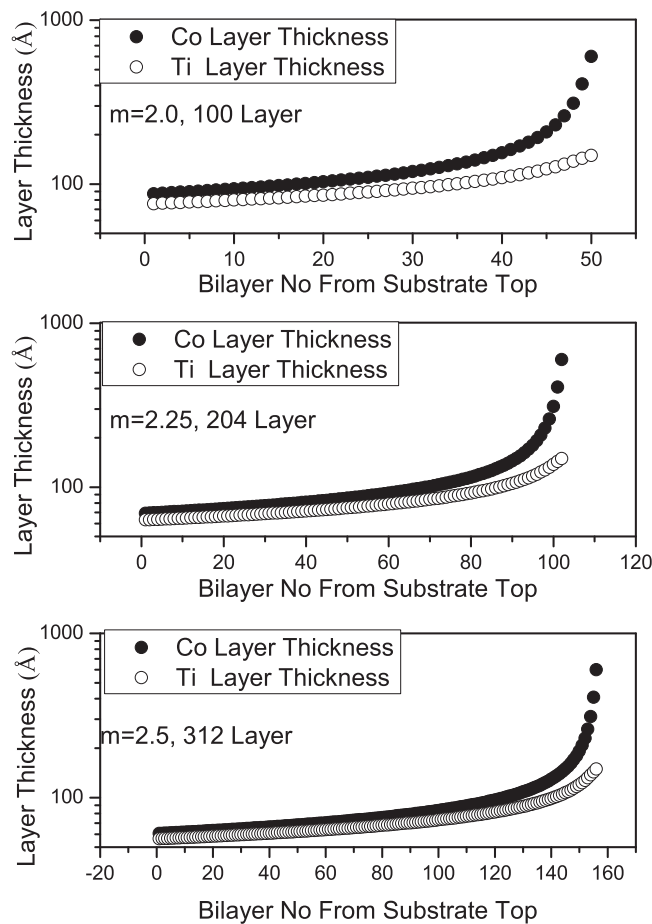


FIG. 11. Designed layer structure of $m = 2.0$, $m = 2.25$, and $m = 2.5$ Co/Ti supermirror polarizer.

the supermirror polarizers have been characterized by measuring Polarized Neutron Reflectivity (PNR) at DHRUVA reactor BARC, India. The PNR measurements have been carried out at a wavelength of 2.5 \AA , the details of the reflectometer have been described previously.⁷ The reflectivity spectra of the supermirrors, both for up-polarised neutrons (R_{\uparrow}) and down-polarised neutrons (R_{\downarrow}) are shown in Fig. 12, which shows that for $m = 2.0$ supermirror, the reflectivity decreases gradually with increase in q_z and at cut-off value of q reflectivity is $\sim 70\%$ which agrees well with the reflectivity pattern obtained by other workers on similar supermirror structures.⁸

However, in case of $m = 2.25$ (204 layers) and $m = 2.5$ (312 layers) supermirrors, we have observed an oscillatory behaviour in reflectivity pattern where reflectivity gradually falls till a q range of $\sim 0.04 \text{ \AA}^{-1}$ and increases again at higher q range before falling off sharply above the respective critical q value. In order to analyze the cause of this type of unusual variation of reflectivity, the experimentally measured neutron reflectivity spectra of the above two samples are fitted with theoretically generated spectra. However, fitting of such reflectivity spectrum with standard fitting algorithm is quite impossible because of the large number of fitting parameters, i.e., density and thickness of each layer, roughness of each interface, etc. Thus, the experimental reflectivity patterns have been tried to be simulated with by varying the parameters manually in the in-house developed theoretical re-

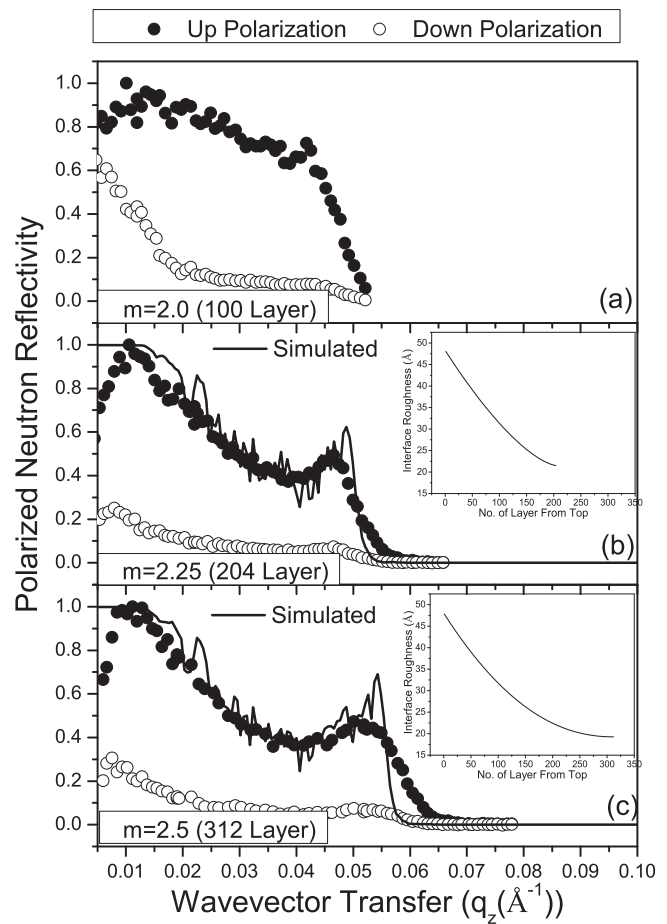


FIG. 12. Polarized neutron reflectivity of (a) $m = 2.0$, (b) $m = 2.25$, and (c) $m = 2.5$ Co/Ti supermirror polarizer. The interface roughness variation with layer no. required to fit the PNR spectra of the respective supermirrors are shown in the inset of (b) and (c).

fectivity simulation code described above. Several iterations have been carried out by incorporating errors in thickness in a particular layer or a set of layers, by dropping a layer from the stack, etc. However, a reflectivity pattern similar to the experimental one could only be generated when a variable interface roughness is introduced in the multilayer stack in such a way that it increases from layers with lower thickness to layers with higher thickness in a certain fashion. The theoretically generated PNR spectrum of spin-up neutrons for $m = 2.25$ (204 layers) supermirror having stepwise variation of interface roughness from 20 \AA to 50 \AA with nominal layer thickness structure is shown (straight line) in Fig. 12(b) along with the experimental data. In the inset of Fig. 12(b) the polynomial fit of the variation of interface roughness with layer number is shown. Similarly in Fig. 12(c) the theoretically generated PNR spectrum of spin-up neutrons for $m = 2.5$ (312 layers) supermirror is shown as a straight line along with the experimental data. Here the interface roughness is varied stepwise from 17 \AA to 50 \AA keeping the nominal layer thickness structure, in the inset of Fig. 12(c) the polynomial fit of this roughness variation with layer number is shown. So it is concluded from these two spectra that the interface roughness values for $m = 2.25$, and $m = 2.5$ supermirrors are quite high which is responsible for the unusually oscillatory behaviour in the reflectivity spectra of neutrons.

However from the X-ray reflectivity measurement of the Co/Ti periodic multilayers, shown in Fig. 8, it is found that even for periodic multilayer of 176 Å bilayer thickness the interface roughness is ~ 10 Å. So the high value of interface roughness observed in the PNR spectra of the above two supermirrors might be due to magnetic roughness at Co/Ti interface. Similar observations had also been made by Scharpf *et al.*¹⁸ for their Co/Ti supermirror deposited by evaporation technique. Diffusion of Co into Ti layer creates a nonmagnetic layer at the Co–Ti interface which leads to reduction in magnetic contrast at the interface. Senthil Kumar *et al.*³³ have shown that for FeCoV/Ti multilayer also two magnetic phases exist in the magnetic layer, one in the bulk region and other at the interface, magnetic moment at the interface being less than that inside the bulk. Due to mixing or alloy formation at the interface, this region behaves almost like a nonmagnetic material. This is known as magnetic roughness which increases the total interface roughness.¹⁸ In this context Smardz *et al.*³⁴ had studied the variation of magnetization of Co layers in Co/Ti multilayer samples having different Co layer thicknesses, where they have observed that Co layers get fully magnetized like bulk samples only if the thicknesses of the layers are more than a certain cut-off value. It seems that for Co layers having thickness lower than this, the interface effect dominates and magnetic moments of all Co atoms do not get aligned to the external field.

In order to decrease such magnetic roughness in the interface of magnetic/nonmagnetic materials, two techniques have generally been reported in the literature, viz., (i) compensating the non-magnetic region at Co/Ti interface by increasing Co layer thickness by small amount and decreasing Ti layer thickness by similar amount in each bilayer¹⁸ for keeping the bilayer thickness same or (ii) preventing the diffusion of Co into Ti layer by depositing Co layers under a mixed ambient of argon and air. Such a reactive sputtering process might decrease the grain size of the Co layer which in-turn decreases the inter diffusion at the interface.^{13–15} Scharpf *et al.*¹⁹ had reported improvement of reflectivity of evaporated $m = 1.5$ (80 layers) Co/Ti supermirror by increasing thickness of each Co layers by 10% and decreasing thickness of each Ti layers by 10%. They have also reported¹⁸ improvement of reflectivity of $m = 2.5$ (300 layers) Co/Ti polarizing supermirror by increasing each Co layer thickness by 7 Å and decreasing each Ti layer thickness by 7 Å. In both the above cases the authors have vented the deposition system periodically, which according to them has helped in obtaining better reflectivity for the supermirrors. On the other hand Senthil Kumar *et al.*¹⁵ had demonstrated improvement of reflectivity of Ni/Ti multilayer and $m = 3.65$ (600 layers) Ni/Ti supermirrors by reactive sputtering of Ni layer with synthetic air in their dc magnetron sputtering system.

We have deposited $m = 2.25$ (204 layers) and $m = 2.5$ (312 layers) Co/Ti supermirror polarizers adopting both the above techniques and the measured PNR spectra of the samples are shown in Fig. 13. It can be noticed that in all the four cases, the reflectivity spectra do not show the unusually oscillatory behavior as observed in Figs. 12(b) and 12(c). In the case of compensation technique, we have increased the thickness of each Co layer by 10 Å and de-

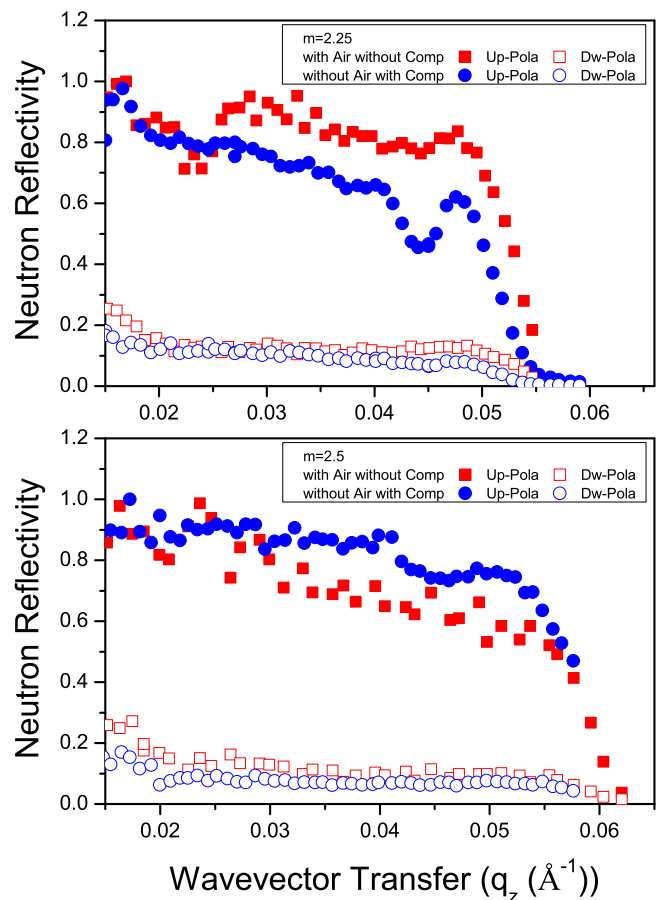


FIG. 13. Polarized neutron reflectivity of $m = 2.25$ and $m = 2.5$ supermirrors deposited with air without compensation layer thickness and without air with compensation layer thickness.

crease the thickness of each Ti layer by 10 Å. In the other set, we have deposited each Co layer of the supermirror with an optimized air flow rate of 20 ml m^{-1} during the sputtering process. It has been observed that higher air flow causes significant oxidation of Co layers leading to drastic reduction in the reflectivity of the supermirror while lower air flow does not have much effect in improving the quality of the interface. The above four supermirrors are also found to yield reasonably good reflectivity ($\sim >60\%$) at the critical values of wavevector transfer (q) and the polarization efficiency ($\frac{R_{\uparrow} - R_{\downarrow}}{R_{\uparrow} + R_{\downarrow}}$) of the supermirror polarizers are estimated to be $\sim 85\%$. However the measured polarization efficiency of the supermirrors is also limited by the flipper efficiency of neutron reflectometer used in this study which is $\sim 90\%$ and hence actual polarization efficiency of the supermirrors would be higher than this. It should also be noted that in Fig. 13, the reflectivity spectrum of up-polarised neutrons of the $m = 2.25$ supermirror deposited with a compensating Co layer thickness has a dip in high q range while that of the supermirror deposited with mixed ambient of air and argon has a dip at a low q range. These aberrations are due to some missing layers which occurred due to accidental problems during deposition of the supermirrors and are not really intrinsic characteristics of the supermirrors.

It should also be noted that for the $m = 2.25$ and $m = 2.5$ Co/Ti supermirrors described above, nonalignment of magnetic moments at the interface of thin Co layers not only increases the magnetic roughness of those layers but also increases the magnetic roughness of thicker layers. Due to this, the magnetic roughnesses at the interface of thicker Co and Ti layers of $m = 2.25$ and $m = 2.5$ supermirrors are higher than that of interface of similar layers for the $m = 2.0$ supermirror.

CONCLUSION

A 9 m long in-line dc sputtering system has been developed in-house for deposition of neutron supermirrors on large size substrates and in large numbers for applications in various neutron based experiments. The coating system has provisions for *in situ* to-and-fro substrate scanning mechanism during deposition, so an area of 1500 mm \times 150 mm can be deposited uniformly with a thickness variation of <5%. The system is equipped with a load-lock chamber and all other essential gadgets required for good quality thin film deposition and single layer metallic films of Co and Ti with very low roughness and bulk-like density could be prepared in this system. All the gadgets have been interfaced with computer and a robust process control software has been developed so that multilayer thin films with more than 500 layers can be deposited with ease as per a user-defined design within a reasonable time frame. Subsequent to optimisation of various process parameters, viz., magnetron power, rate of deposition, speed of substrate trolley, etc., Co/Ti based thin film multilayer supermirror polarizers of up to $m = 2.5$ have been fabricated successfully in the above in-line sputtering system, which shows high reflectivity up to a reasonably large critical wavevector transfer (q) of $\sim 0.06 \text{ \AA}^{-1}$. It has been observed that use of a mixed ambient of argon and air while depositing Co layers or increasing the Co layer thickness from its nominal value by $\sim 10 \text{ \AA}$ improves the reflectivity pattern of the supermirrors significantly. The computer code for designing these supermirrors and simulating the neutron reflectivity pattern has also been developed in-house.

ACKNOWLEDGMENTS

The authors acknowledge Dr. S. L. Chaplot, Director, Physics Group, BARC and Dr. R. Mukhopadhyay, Head, Solid State Physics Division, BARC for their keen interest in the above work.

- ¹G. L. Squires, *Introduction to Thermal Neutron Scattering* (Dover Publications, New York, 1996).
- ²*X-ray and Neutron Reflectivity Principles and Applications*, Lecture Notes in Physics Vol. 770, edited by J. Daillant and A. Gibaud (Springer, Berlin, 2009).
- ³R. K. Crawford, "Neutron scattering instrumentation – A guide to future directions," *Proceedings of ICANS-XV*, pp. 61–68, 2000.
- ⁴D. Liua, M. V. Gubarev, G. Resta, B. D. Ramsey, D. E. Monctona, and B. Khaykovicha, *Nucl. Instrum. Meth. Phys. Res. A* **686**, 145–150 (2012).
- ⁵F. Mezei, *Commun. Phys.* **1**, 81–85 (1976).
- ⁶M. Nagano, H. Takai, D. Yamazaki, R. Maruyama, K. Soyama, and K. Yamamura, *J. Phys.: Conf. Ser.* **251**, 012077 (2010).
- ⁷S. Singh and S. Basu, *Pramana – J. Phys.* **63**(2), 387–391 (2004).
- ⁸J. R. Stewart, P. P. Deen, K. H. Andersen, H. Schober, J. F. Barthelemy, J. M. Hillier, A. P. Murani, T. Hayes, and B. Lindenau, *J. Appl. Crystallogr.* **42**, 69–84 (2009).
- ⁹P. Fouquet, B. Farago, K. H. Andersen, P. M. Bentley, G. Pastrello, I. Sutton, E. Thaveron, F. Thomas, E. Moskvina, and C. Pappas, *Rev. Sci. Instrum.* **80**, 095105 (2009).
- ¹⁰F. Mezei and P. A. Dagleish, *Commun. Phys.* **2**, 41–43 (1977).
- ¹¹R. Maruyama, D. Yamazaki, T. Ebisawa, and K. Soyama, *Nucl. Instrum. Meth. Phys. Res. A* **600**, 68–70 (2009).
- ¹²M. Hino, H. Hayashida, M. Kitaguchi, Y. Kawabata, M. Takeda, R. Maruyama, T. Ebisawa, N. Torikai, T. Kume, and S. Tasaki, *Physica B* **385–386**, 1187–1189 (2006).
- ¹³O. Elsenhans, P. Boni, H. P. Friedli, H. Grimmer, P. Buffat, K. Leifer, J. Sochtig, and I. S. Anderson, *Thin Solid Films* **246**, 110–119 (1994).
- ¹⁴P. Hoghoj, I. Anderson, R. Siebrecht, W. Graf, and K. Ben-Saidane, *Physica B* **248**, 355–359 (1999).
- ¹⁵M. Senthil Kumar, P. Boni, and M. Horisberger, *Nucl. Instrum. Meth. Phys. Res. A* **529**, 90–93 (2004).
- ¹⁶H. Ju and B. J. Heuser, *Appl. Phys. Lett.* **90**, 073113 (2007).
- ¹⁷D. Clemens, P. Boni, H. P. Friedli, R. Götzel, C. Fermon, H. Grimmer, H. van Swygenhoven, J. Archer, F. Klöse, Th. Krist, F. Mezei, and P. Thomas, *Physica B* **213–214**, 942–944 (1995).
- ¹⁸O. Scharpf and I. S. Anderson, *Physica B* **198**, 203–212 (1994).
- ¹⁹O. Scharpf, *Physica B* **156–157**, 639–646 (1989).
- ²⁰V. G. Syromyatnikov, A. Menelle, Z. N. Soroko, and A. F. Schebetov, *Physica B* **248**, 355–357, (1998).
- ²¹A. Biswas, Sk. Maidul Haque, J. Misal, K. D. Lagoo, R. D. Veerapur, M. Padmanabhan, R. K. Puri, R. Sampathkumar, Ajaya Kumar, D. Bhattacharya, D. Bhattacharyya, and N. K. Sahoo, *AIP Conf. Proc.* **1591**, 985–987 (2014).
- ²²Ph. Houdy, *Rev. Phys. Appl.* **23**, 1653 (1988).
- ²³A. Biswas and D. Bhattacharyya, *J. Appl. Phys.* **109**, 084311 (2011).
- ²⁴S. Maidul Haque, A. Biswas, D. Bhattacharyya, R. B. Tokas, D. Bhattacharyya, and N. K. Sahoo, *J. Appl. Phys.* **114**, 103508 (2013).
- ²⁵B. Yang, L. J. Piliore, J. E. Yehoda, K. Vedam, and R. Messier, *Phys. Rev. B* **36**(11), 6206–6208 (1987).
- ²⁶A. G. Gukasov, V. A. Ruban, and M. N. Bedrizova, *Sov. Tech. Phys. Lett.* **3**, 52–53 (1977).
- ²⁷S. Yamada, T. Ebisawa, N. Achiwa, T. Akiyoshi, and S. Okamoto, *Annu. Rep. Res. React. Inst., Kyoto Univ.* **11**, 8–27 (1978).
- ²⁸J. Schelten and K. Mika, *Nucl. Instrum. Meth.* **160**, 287–294 (1979).
- ²⁹O. Scharpf, *AIP Conf. Proc.* **89**, 182–189 (1982).
- ³⁰J. B. Hayter and H. A. Mook, *J. Appl. Crystallogr.* **22**, 35–41 (1989).
- ³¹N. K. Pleshanov, *Nucl. Instrum. Meth. Phys. Res. A* **524**, 273–286 (2004).
- ³²I. G. Parrat, *Phys. Rev.* **95**, 359 (1954).
- ³³M. Senthil Kumar, V. R. Shah, C. Schanzer, P. Boni, T. Krist, and M. Horisberger, *Physica B* **350**, E241–E244 (2004).
- ³⁴K. Smardz, L. Smardz, and A. Jezierski, in *Proceedings of the European Conference "Physics of Magnetism '99," Acta Physica Polonica A* **97**(3), 507 (2000).